Thermodynamics of The $Pd_{43}Ni_{10}Cu_{27}P_{20}$ Bulk Metallic Glass Forming Alloy

Masahiro Kuno, Ludi A. Shadowspeaker, Jan Schroers[1], and Ralf Busch
Department of Mechanical Engineering, Oregon State University, Corvallis Oregon 97331
[1]Keck Laboratory of Engineering Materials, California institute of technology, Pasadena, CA 91125

ABSTRACT

The thermodynamics of the bulk metallic glass forming $Pd_{43}Ni_{10}Cu_{27}P_{20}$ alloy were investigated with differential scanning calorimetry (DSC). The specific heat capacity of the undercooled liquid with respect to the crystalline mixture was measured in the DSC simultaneously with the enthalpy of crystallization over the entire supercooled liquid region. The enthalpy, entropy, and Gibbs free energy change between the liquid and the crystalline mixture was determined from the specific heat capacity data. The calculated enthalpy function closely matched the enthalpies of crystallization that were measured in the DSC, which verifies the validity of the thermodynamic model used. A small Gibbs free energy difference between undercooled liquid and crystalline mixture was found for decreasing temperature in $Pd_{43}Ni_{10}Cu_{27}P_{20}$ when compared to other glass forming alloys. This reflects a small driving force for crystallization when undercooling this alloy and is the main contributing factor for it's high glass forming ability.

INTRODUCTION

Multicomponent glass forming alloy families such as La-Al-Ni [1], Mg-Cu-Y [2], Zr-Ti-Cu-Ni-Be [3], and Zr-Ni-Al-Cu [4], exhibit very good glass forming ability. These bulk metallic glasses (BMG) show high thermal stability with respect to crystallization, which allows for detailed studies of their thermodynamic properties in the undercooled liquid state. An essential thermodynamic property is the specific heat capacity, c_p, of the undercooled liquid because, when referenced to the c_p of the crystal, the thermodynamic functions of enthalpy, entropy and Gibbs free energy can be derived by well-defined integration functions [5]. This study focuses on the thermodynamics of the $Pd_{43}Ni_{10}Cu_{27}P_{20}$ BMG [6]. This alloy has a lower critical cooling rate, when processed in B_2O_3 [7], than the other Pd-Ni-P based alloys that have been studied so far [8]. The goal of this investigation is to measure the specific heat capacity and the enthalpy of crystallization of undercooled $Pd_{43}Ni_{10}Cu_{27}P_{20}$ as a function of temperature and compare the experimental enthalpy change with the enthalpy change that can be calculated from the specific heat capacity difference between undercooled liquid and crystalline mixture.

EXPERIMENTAL METHODS

$Pd_{43}Ni_{10}Cu_{27}P_{20}$ ingots were prepared from a mixture of the elements with a purity ranging from 99.0% to 99.999% by induction melting in quartz tubes. To obtain glass, the melt was held at 1200 K for 1200 s and then quenched in water. The samples were fluxed with B_2O_3 during this procedure to prevent crystallization. Glassy $Pd_{43}Ni_{10}Cu_{27}P_{20}$ samples up to 70 mg and an additional 3 to 5 mg of flux were introduced into graphite crucibles and analyzed in a Perkin-Elmer DSC7.

The absolute values of the specific heat capacity of the glassy sample up to 600 K, the crystallized samples up to 770 K, and the liquid from 650 to 950 K were determined in

reference to the specific heat capacity of a sapphire standard. The experiments were done in heating experiments for the glass and the crystal and in undercooling experiments for the liquid. Crystallization can not be avoided on heating but on cooling. Therefore we performed the measurements on the liquid upon cooling, Figure 1 shows a typical heating experiment upon heating. The sample was first heated from

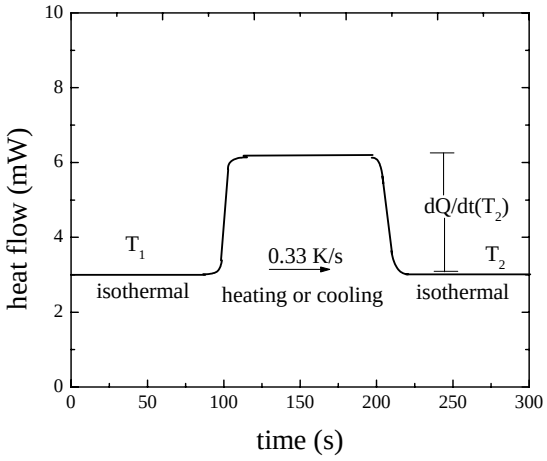

Figure 1: Typical heat flow versus time signal for a heat capacity measurement in the DSC.

temperature T_1 to temperature T_2 with a constant rate of 0.33 Ks^{-1} and held isothermally for 120 s. This resulted in a step of the heat flux d*Q*/dt like the one shown in Fig. 1. This step can be described by the equation

$$\frac{dQ}{dt} = \left(\frac{dQ}{dt}\right)_{\dot{T}\neq 0} - \left(\frac{dQ}{dt}\right)_{\dot{T}=0} = C \cdot \frac{dT}{dt} \qquad (1),$$

where $(dQ/dt)_{\dot{T}\neq 0}$ is the power necessary to heat the sample and container with overall heat capacity *C* and hold it at T_2, and $(dQ/dt)_{\dot{T}=0}$ is the power which is needed to just keep the temperature constant [5]. To determine the absolute specific heat capacity of the sample, the heat capacities of the empty sample container and of the sapphire standard were also measured.

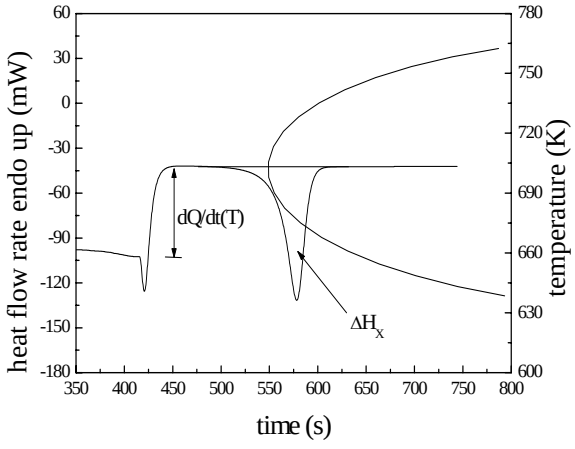

Figure 2: Combined specific heat capacity and isothermal crystallization experiment, measuring the enthalpy of crystallization. The time-temperature-transformation curve is also shown in this schematic.

The specific heat capacity of the sample was then calculated with the equation

$$c_p(T)_{sample} = \frac{\dot{Q}_{sample} - \dot{Q}_{pan}}{\dot{Q}_{sapphire} - \dot{Q}_{pan}} \cdot \frac{m_{sapphire} \cdot \mu_{sample}}{m_{sample} \cdot \mu_{sapphiree}} \cdot c_p(T)_{sapphire} \quad (2),$$

where m_i is the mass, μ_i the mole mass, and $c_p(T)_{sapphire}$ the specific heat capacity of sapphire {5].

In Fig. 2 a typical experimental curve of an undercooling experiment is shown. The sample is first melted and then undercooled to the assigned isothermal temperature. Once that is reached, we observe the step in heat flux that is proportional to the heat capacity. Subsequently, the enthalpy of crystallization, ΔH_x, is measured directly in the same experiment. The heat of crystallization is obtained by integrating the exothermic peak .

RESULTS

The specific heat capacities of the $Pd_{43}Ni_{10}Cu_{27}P_{20}$ alloy in the glassy, crystalline, and supercooled liquid states are shown in Fig.3. T_g indicates the glass transition temperature, which can be defined as the onset of the endothermic heat event in the DSC. T_k is the Kauzmann temperature, which is defined as the theoretical temperature at which the entropy of the undercooled liquid is equal to the entropy of the crystal [9], and T_m is the melting temperature.

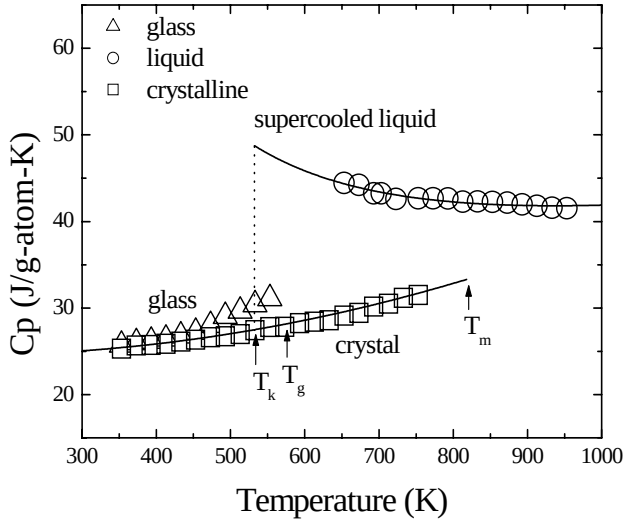

Figure 3: The specific heat capacity, c_p, of $Pd_{43}Ni_{10}Cu_{27}P_{20}$. The fits of Eqs. 3 and 4 are plotted as lines on the graph. T_g, T_k, and T_m are the glass transition, Kauzmann, and melting temperature respectively.

The temperature dependence of c_p for the undercooled liquid far above the Debye temperature can be expressed as

$$c_p(T) = 3R + a \cdot T + b \cdot T^{-2} \quad (3),$$

where a and b are constants, R is the universal gas constant, 8.31 $J \cdot (g\text{-atom})^{-1} \cdot K^{-1}$, and T is the temperature[10] .

On the other hand, c_p of the crystal is described with the equation

$$c_p(T) = 3R+c\cdot T+d\cdot T^2 \qquad (4),$$

where c and d are constants. These equations were fitted to the data in Fig. 3 and the constants were found to be a = 0.012, b = $4.9\cdot10^6$, c = 0.0053, and d = $1.9\cdot10^{-5}$ in the appropriate units. These fitted curves are plotted as lines in Fig. 3.

From the measured c_p data it is possible to calculate the thermodynamic functions for the $Pd_{43}Ni_{10}Cu_{27}P_{20}$ alloy as a function of temperature. The Gibbs free energy of the undercooled liquid with respect to the crystal, $\Delta G_{l-x}(T)$, can be calculated by integrating the specific heat capacity difference according to the equation

$$\Delta G_{l-x}(T) = \Delta H_f - \Delta S_f \cdot T - \int_T^{T_f} \Delta c_p{}^{l-x}(T')dT' + T\int_T^{T_f} \frac{\Delta c_p{}^{l-x}(T')}{T'}dT' \qquad (5),$$

where ΔH_f and ΔS_f are the enthalpy and entropy of fusion at the temperature T_f, respectively [5]. T_f is the temperature where the Gibbs free energy of the liquid and crystal are equal. Since the melting peak is relatively sharp, T_f is well approximated by the peak melting temperature (815 K) as observed in the DSC.

DISCUSSION

The enthalpies, entropies and Gibbs free energies were calculated using equation 5. The entropy curve (not shown) yields the Kauzmann temperature 530 K Figure 4 shows the calculated enthalpy curve of the liquid with respect to the crystal $\Delta H_{l-x}(T)$ that has been calculated from the heat of fusion and integration the the specific heat capacity difference between crystal and liquid as a solid line. In comparison the experimental heats of crystallization for numerous measurements are plotted as open circles. The heats of crystallization were obtained in the DSC for different undercoolings in the entire range of the undercooled liquid. It is evident in Fig. 4, that there is an excellent agreement between the experimentally determined enthalpies and the enthalpy function that was calculated from the fitted c_p curves. This agreement verifies the fit parameters of Eqs. 3 and 4 as well as the T_f value in Eq. 5 that were used to determine the entropy and Gibbs free energy functions of the alloy.

In Fig. 5, the Gibbs free energy difference between the supercooled liquid and the crystalline mixture for $Pd_{43}Ni_{10}Cu_{27}P_{20}$ is compared to other glass forming systems [11]. The critical cooling rates, R_c, for the alloys are also shown in Fig. 5. R_c ranges between 1 Ks^{-1} for $Zr_{41.2}Ti_{13.8}Cu_{12.5}Ni_{10}Be_{22.5}$ and 10^4 Ks^{-1} for $Zr_{62}Ni_{38}$. The glass formers with lower R_c values have smaller Gibbs free energy differences with respect to the crystalline state than the glass formers with higher values of R_c, because the smaller driving force for crystallization result in slower nucleation kinetics and shift the time-temperature diagram to longer times. It is important to note that the $Pd_{43}Ni_{10}Cu_{27}P_{20}$, has an extremely low critical rate of 0.09 K/s. This must be directly connected with the small Gibbs free energy difference between undercooled liquid and crystalline mixture in this alloy compared to all other alloys. In fact, as can be seen in Fig. 4, the alloy has a very small enthalpy of fusion of only about 5 KJ/g-atom, which is rather comparable to a value for an enthalpy of crystallization close to Tg in most other glass former. This means that it also has a small entropy of fusion. This explains the small Gibbs free energy difference between liquid and crystalline mixture, since the negative slope of the Gibbs free energy curve at the melting point corresponds to the entropy of fusion. The small entrpies of fusion indicate strong short range order in the melt.

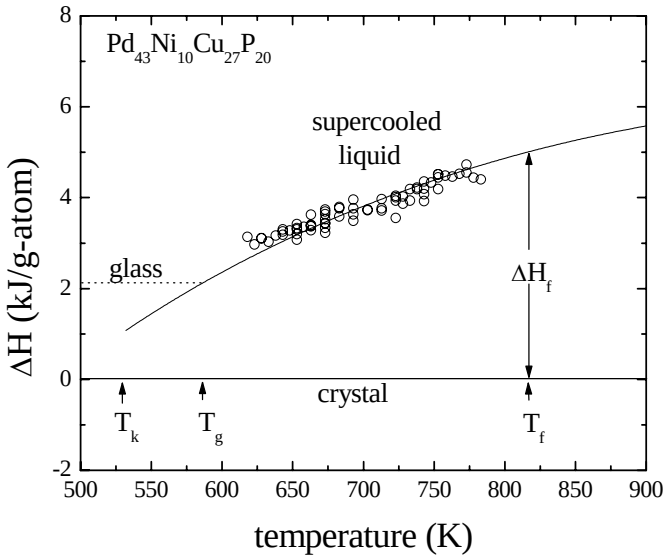

Figure 4: Calculated enthalpy of the undercooled liquid with respect to the crystal for $Pd_{43}Ni_{10}Cu_{27}P_{20}$ as a function of temperature (solid curve). The open circles represent the enthalpy difference that was directly measured in the DSC with the heat of crystallization at the different temperatures.

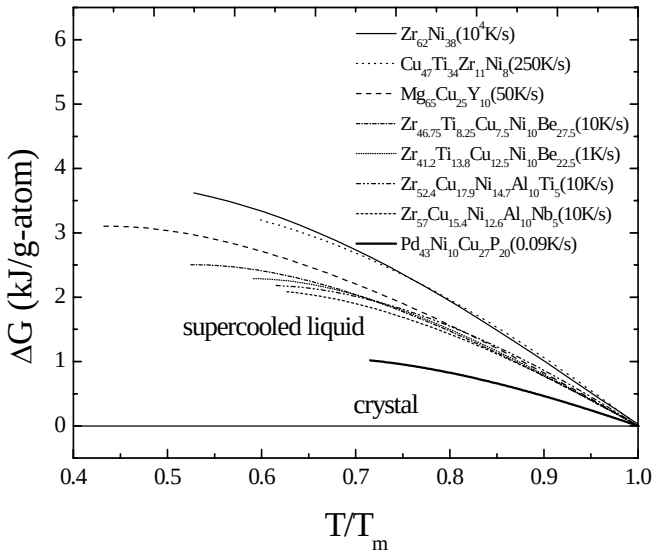

Figure 5: The Gibbs free energy difference between the liquid and crystalline states for a number of metallic glass forming alloys including $Pd_{43}Ni_{10}Cu_{27}P_{20}$. The data are normalized by the melting temperatures of the alloys. The critical cooling rates of the alloys are also listed.

CONCLUSIONS

A differential scanning calorimeter was used to measure the specific heat capacity of the $Pd_{43}Ni_{10}Cu_{27}P_{20}$ alloy in the glassy, crystalline, and liquid state. The thermodynamic functions of enthalpy, entropy, and Gibbs free energy were calculated using the difference in specific heat capacity between the liquid and crystal, and there is very good agreement between the calculated enthalpy as a function of temperature and the enthalpies that were measured directly in the DSC. The small Gibbs free energy difference between the liquid and the crystal reflects a small driving force for crystallization, which indicates high glass forming ability for this alloy. The underlying reason for this is the very small entropy of fusion. This suggests a large degree of short range order in the liquid

ACKNOWLEDGEMENTS

The authors thank W. L. Johnson for fruitful discussions. This work was supported by DARPA (Grant no. DAAD-19-01-1-0525).

REFERENCES

[1] A. Inoue, T. Zhang, and T. Masumoto, Mater. Trans., JIM **31**, 425 (1991).
[2] A. Inoue, A. Kato, T. Zhang, S. G. Kim, and T. Masumoto, Mater. Trans., JIM **32**, 609 (1991).
[3] A. Peker and W. L. Johnson, Appl. Phys. Lett., **63**, 2342 (1993).
[4] T. Zhang, A. Inoue, and T. Masumoto, Mater. Trans., JIM **32**, 1005 (1991).
[5] R. Busch, W. Lui, and W. L. Johnson, J. Appl. Phys., **83**, 4134 (1998).
[6] L. Lu, G. Wilde, G. P. Gorler, and R. Willnecker, J. Non-Cryst. Sol., **251**, 577 (1999).
[7] H. W. Kui, A. L. Greer, and D. Turnbull, Appl. Phys. Lett., **45**, 615, (1984).
[8] J. Schroers, Y. Wu, R. Busch, and W. L. Johnson, Acta Mater., **49,** 2773 (2001).
[9] W. Kauzmann, Chem. Rev. 43, **219**, (1948).
[10] O. Kubaschewski, C. B. Alcock, and P. J. Spencer, *Materials Thermochemistry*, 6th ed. (Pergamon, New York, 1993).
[11] R. Busch, E. Bakke, and W. L. Johnson, Mater Sci. Forum, **235-238**, 327 (1996).